Sensitivity Improvement in Multi-Dimensional NMR Spectroscopy

Mark Rance

Department of Molecular Biology
The Scripps Research Institute
10666 North Torrey Pines Road
La Jolla, California 92037 U.S.A.

Contents

I. Introduction

A critical concern in many applications of nuclear magnetic resonance spectroscopy is the sensitivity of the measurements, as determined by the achievable signal-to-noise ratio for a given experiment duration. The sensitivity of a NMR measurement is affected by many factors (1-3), and numerous schemes have been described over the years for improving the sensitivity. These schemes can generally be categorized into one or more of three broad areas: (i) modification of experimental techniques (i.e. spin physics); (ii) advancements in spectrometer hardware; and (iii) utilization of new data processing procedures. The present paper describes a novel methodology, falling under category (i), for providing a factor of up to $\sqrt{2}$ improvement in sensitivity for a variety of multi-dimensional NMR experiments. The principle upon which this new methodology is based will be reviewed below, followed by a brief description of a few practical applications.

II. Theory

In order to explain the basis of the sensitivity improvement scheme for multi-dimensional NMR spectroscopy, it would perhaps be useful first to mention a somewhat analogous method which involves a hardware modification rather than a direct manipulation of the spin system, and is applicable in any NMR experiment. Some time ago Hoult and coworkers (4) pointed out that, at least in principle, a $\sqrt{2}$ improvement in sensitivity can be achieved in NMR measurements by using two orthogonal detection coils rather than the single coil normally employed. If the two rf coils are orthogonally positioned but otherwise identical, the NMR signals

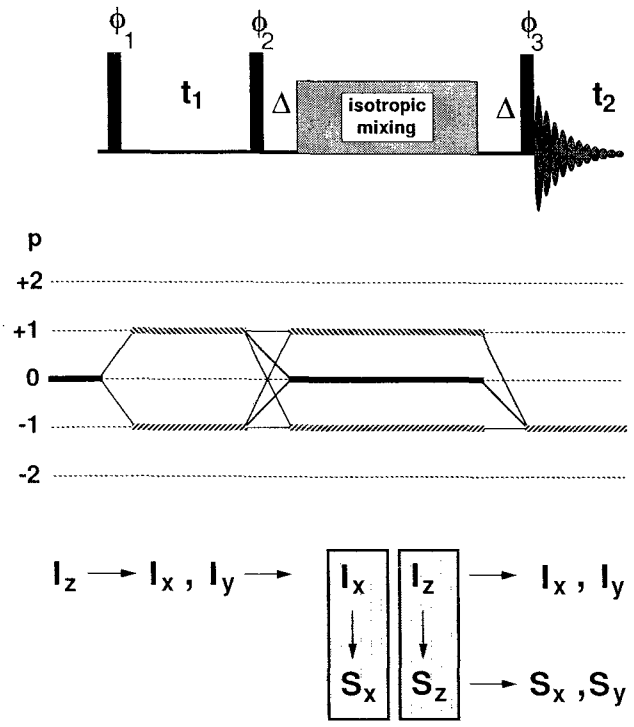

Figure 1: Pulse sequence, a diagram of the coherence transfer pathway, and the relevant density operator terms for a sensitivity-enhanced 2D TOCSY experiment (34). The pulse sequence itself is identical to the z-filtered TOCSY experiment in common use (8,9); the sensitivity enhancement is achieved by separating the conventional phase-cycling into two halves and recording the data separately.

detected in each will be identical except for a relative phase shift of 90°; thus, after correcting for the relative phase shift, the two NMR signals can be combined to double the size of the detected signal. On the other hand, the thermal noise generated in the two receiver circuits (probe coils plus preamplifiers) will be statistically independent, and thus when combined will increase the rms noise voltage by only a factor of $\sqrt{2}$. The net result of this scheme therefore is a $\sqrt{2}$ improvement in the overall sensitivity of the NMR experiment. Unfortunately, this concept has been difficult to implement due to practical problems in designing an efficient, crossed-coil probe. The sensitivity improvement scheme described below is essentially an analogue of cross-coil detection for evolution periods (5) in multi-dimensional NMR experiments.

To explain the basic principle underlying the sensitivity enhancement scheme, the response of an isolated spin-1/2 nucleus to the pulse sequence shown in Figure 1 will be described; application of this pulse sequence to a coupled spin system produces a 2D TOCSY spectrum (6-9), but for present purposes it can be viewed as simply producing a 2D chemical shift-resolved spectrum of the uncoupled spin-1/2 nuclei. All relaxation effects are ignored. Starting from the equilibrium magnetization of the spin-1/2, the first 90°_x pulse creates transverse magnetization which then evolves under the influence of the chemical shift/resonance offset, Ω, to:

$$\sigma(t_1) = I_x \sin \Omega t_1 - I_y \cos \Omega t_1 \qquad (1)$$

where for convenience the single spin angular momentum operators are used to indicate the relevant state of the spin system, and constants of proportionality have been omitted. The $90^\circ_{\phi_2}$ pulse at the beginning of the mixing period produces the following:

$$\sigma_a(t_1, \tau_m = 0) = I_x \sin \Omega t_1 + a I_z \cos \Omega t_1 \qquad (2)$$

where $a = -1$ for $\phi_2 = +x$ and $a = +1$ for $\phi_2 = -x$. Assuming for the moment that some arbitrary pulse sequence is applied during the mixing period τ_m, the state of the spin system just prior to the last 90°_x pulse can be written in general terms as:

$$\begin{aligned}\sigma_a(t_1, \tau_m) = {} & [I_x f_x(\tau_m) + I_y f_y(\tau_m) + I_z f_z(\tau_m)] \sin \Omega t_1 \\ & + a[I_x g_x(\tau_m) + I_y g_y(\tau_m) + I_z g_z(\tau_m)] \cos \Omega t_1 \end{aligned} \qquad (3)$$

where the functions $f_\beta(\tau_m)$ and $g_\beta(\tau_m)$ express the net effect of the mixing sequence on the I_x and I_z components, respectively. The last 90°_x pulse generates the following:

$$\begin{aligned}\sigma_a(t_1, \tau_m, t_2 = 0) = {} & [I_x f_x(\tau_m) - I_y f_z(\tau_m)] \sin \Omega t_1 \\ & + a[I_x g_x(\tau_m) - I_y g_z(\tau_m)] \cos \Omega t_1 \end{aligned} \qquad (4)$$

where unobservable I_z terms have been dropped. Finally, precession due to the chemical shift or resonance offset during the detection period will produce the following result:

$$\sigma_a(t_1,\tau_m,t_2) =$$
$$I_x[(f_x(\tau_m)\cos\Omega t_2 + f_z(\tau_m)\sin\Omega t_2)\sin\Omega t_1$$
$$+a(g_x(\tau_m)\cos\Omega t_2 + g_z(\tau_m)\sin\Omega t_2)\cos\Omega t_1]$$
$$+I_y[(f_x(\tau_m)\sin\Omega t_2 - f_z(\tau_m)\cos\Omega t_2)\sin\Omega t_1$$
$$+a(g_x(\tau_m)\sin\Omega t_2 - g_z(\tau_m)\cos\Omega t_2)\cos\Omega t_1] \quad (5)$$

Inspection of eqn. 5 indicates that for some arbitrary mixing sequence, a 2D Fourier transformation of the time-domain NMR signal will result in complicated lineshapes in the 2D spectrum.

To proceed, assume that instead of some arbitrary mixing sequence being applied, a so-called 'isotropic' sequence is employed (6). One of the properties of an isotropic mixing sequence is that the total spin angular momentum I_α (α= x,y or z) is conserved (10). Thus, eqn. 5 simplifies to:

$$\sigma_a(t_1,\tau_m,t_2) =$$
$$I_x[f_x(\tau_m)\sin\Omega t_1\cos\Omega t_2 + ag_z(\tau_m)\cos\Omega t_1\sin\Omega t_2]$$
$$+I_y[f_x(\tau_m)\sin\Omega t_1\sin\Omega t_2 - ag_z(\tau_m)\cos\Omega t_1\cos\Omega t_2] \quad (6)$$

2D Fourier transformation of the NMR signal represented by eqn. 6 will still produce spectral peaks with a highly undesirable phase-twist (11,12). This phase twist can be removed, however, if either an additive or subtractive combination is made of the two data sets collected separately for $\phi_2 = +x$ ($a = -1$) and $\phi_2 = -x$ ($a = +1$):

$$\begin{aligned}\sigma^+(t_1,\tau_m,t_2) &= \sigma_{+1}(t_1,\tau_m,t_2) + \sigma_{-1}(t_1,\tau_m,t_2)\\ &= 2I_x[f_x(\tau_m)\sin\Omega t_1\cos\Omega t_2]\\ &\quad +2I_y[f_x(\tau_m)\sin\Omega t_1\sin\Omega t_2] \quad (7a)\end{aligned}$$

$$\begin{aligned}\sigma^-(t_1,\tau_m,t_2) &= \sigma_{+1}(t_1,\tau_m,t_2) - \sigma_{-1}(t_1,\tau_m,t_2)\\ &= 2I_x[g_z(\tau_m)\cos\Omega t_1\sin\Omega t_2]\\ &\quad -2I_y[g_z(\tau_m)\cos\Omega t_1\cos\Omega t_2] \quad (7b)\end{aligned}$$

A complex Fourier transformation with respect to t_2 and a cosine or sine transformation with respect to t_1 of the signals represented by eqns. 7 will produce spectra with the desired pure phase lineshapes, due to the fact that the signals are amplitude-modulated with respect to t_1 instead of phase-modulated (11,12). The additive combination of the two data sets for $\phi_2 = +x$ and $-x$ effectively eliminates the pathway evolving from the I_y term present at the end of the evolution period; likewise, the subtractive combination eliminates the pathway from the I_x term. This phase-cycling procedure is an inherent part of the z-filtered TOCSY experiment (8,9); usually, the subtractive combination of eqn. 7b is chosen for practical reasons (8). A popular alternative to phase-cycling for generating amplitude-modulated signals in TOCSY experiments is the use of 'trim' pulses and/or non-isotropic mixing sequences to eliminate one of the orthogonal magnetization components present at the end of the evolution period (7). Discrimination of the sign of the resonance frequencies during the evolution period (13) can be achieved via phase selection pulses and hypercomplex Fourier transformations (12-15) or by the time-proportional phase incrementation scheme (13,16-18).

The NMR signals represented by eqns. 7 can be expressed in an equivalent fashion using complex notation as:

$$\sigma^+(t_1,\tau_m,t_2) = 2f_x(\tau_m)\sin\Omega t_1\exp(i\Omega t_2) \quad (8a)$$

$$\sigma^-(t_1,\tau_m,t_2) = -2ig_z(\tau_m)\cos\Omega t_1\exp(i\Omega t_2) \quad (8b)$$

where the real and imaginary components correspond to the coefficients of I_x and I_y, respectively. Inspection of eqns. 7 or 8 indicates that the NMR signals represented by σ^+ and σ^- have a relative phase shift of 90° in both time dimensions. A 2D Hilbert transformation (19) of the signal σ^- generates the result:

$$\hat{\sigma}^-(t_1,\tau_m,t_2) = -2g_z(\tau_m)\sin\Omega t_1\exp(i\Omega t_2) \quad (9)$$

where the hat symbol is used to represent the 2D Hilbert transformation. The combination of eqns. 8a and 9 yields the following:

$$\begin{aligned}\sigma^c(t_1,\tau_m,t_2) &= \sigma^+(t_1,\tau_m,t_2) - \hat{\sigma}^-(t_1,\tau_m,t_2) \quad (10)\\ &= 2[f_x(\tau_m) + g_z(\tau_m)]\sin\Omega t_1\exp(i\Omega t_2) \quad (11)\end{aligned}$$

If the assumption is made that $f_x(\tau_m) = g_z(\tau_m)$, then eqn. 11 indicates that the combination represented by eqn. 10 leads to a NMR signal with twice the intensity of the signal which would conventionally be obtained, i.e. the signals represented by either eqn. 8a or 8b. It should be emphasized that extending the above analysis to include the steps necessary for frequency discrimination in the indirectly

detected dimension does not affect the conclusion regarding signal intensity. To determine whether or not a sensitivity improvement is realized by the modified experimental procedures it is necessary to consider the behaviour of the spectral noise when making the combination indicated by eqn. 10; it will be shown below that the random noise in σ^+ is uncorrelated to that in σ^-, and thus the combination which doubles the NMR signal intensity only increases the noise by a factor of $\sqrt{2}$, resulting therefore in a $\sqrt{2}$ improvement in sensitivity.

As illustrated by the trivial example described above, the general procedure and requisite conditions for implementing the sensitivity enhanced scheme in a 2D NMR experiment can be stated as follows. The pulse sequence must be designed to retain the signals originating from both of the orthogonal magnetization components, or higher order spin operator terms, generated during the evolution period by the chemical shift interaction; in conventional experiments one of these two components is eliminated either as an inherent feature of the pulse sequence or by specific design to purge the 2D spectrum of undesirable features (12,13). The sensitivity enhancement scheme is applicable only to experiments in which the mixing sequence causes the relevant, orthogonal spin operator terms generated during the evolution period to have sufficiently similar transfer functions to observable magnetization components during the detection period; in the example above this would require that $f_x(\tau_m) \approx g_z(\tau_m)$ so that the data in eqn. 11 would combine constructively to enhance the signal strength. Some experiments are easily adapted to incorporate the sensitivity improvement scheme, such as the z-filtered TOCSY sequence discussed above, while other experiments can be modified to fulfill the necessary conditions. Some pulse techniques, however, have segments which inherently require a unique coherence transfer pathway (20,21), such as 2D lab-frame (22) or rotating-frame (23) NOE experiments (NOESY or ROESY, respectively), and thus the sensitivity enhancement scheme is inapplicable for the evolution periods preceding the 'bottleneck'.

Since the sensitivity enhancement scheme relies on the ability to retain and combine essentially equivalent information from two orthogonal, coherence transfer pathways in a suitable NMR experiment, it will for convenience be referred to below as PEP (Preservation of Equivalent Pathways) technology. Also for convenience much of the discussion will refer to 2D experiments, but it should be realized that the PEP methodology is applicable in experiments of higher dimensionality as well (*vide infra*).

To implement the sensitivity enhancement scheme for a suitable NMR experiment, it is first necessary to ensure that the propagator for the relevant portion of the pulse sequence, i.e. the portion between the relevant evolution period and the detection period, transforms the appropriate, orthogonal spin operator terms present at the end of the evolution period to observable magnetization terms with approximately equal efficiency (but not necessarily along exactly equivalent coherence transfer pathways). To accomplish this it may be necessary to re-design part of the pulse sequence; in a 2D experiment this part consists of just the mixing period, while in experiments of higher dimensionality it is necessary to consider all the intervening mixing and evolution periods. In addition, the PEP scheme requires the elimination of the phase-cycling normally employed to select one of the two relevant, orthogonal spin operator terms at the end of the appropriate evolution period; instead, two experiments are run in which the appropriate selection pulse (e.g. the second 90° pulse in the example above) is inverted in phase between the two experiments and the data sets are accumulated separately. After the acquisition is completed, additive and subtractive combinations of the two raw data sets are made to generate the sine and cosine, amplitude-modulated data sets, as in eqns. 8. These two new data sets can be treated in either of two ways. First, the two data sets can be independently processed to produce separate 2D (or higher dimensional) spectra; as indicated above, there will be a relative phase shift of 90° in both frequency dimensions (detection dimension and relevant, indirect dimension), and it is therefore necessary to correct for this relative phase shift. The two spectra can then be added together to enhance the signal intensity. While this first procedure for handling the data provides the ability for spectral editing in some heteronuclear experiments (*vide infra*), it is often more convenient to do all of the required data manipulation on the time domain data. The 90° phase shift in the detection dimension of either the additive or subtractive data set is

trivially accomplished by simply interchanging the real and imaginary parts of the complex free induction decays. If the data has been collected using the so-called 'hypercomplex' (12-15) method for sign discrimination in the relevant, indirectly detected frequency dimension, then the necessary 90° phase shift in this dimension is trivially accomplished by swapping the two free induction decays collected for each time increment (i.e. t_1 point in a 2D experiment) as part of the 'hypercomplex' procedure; this swap is usually done on the same data set, either additive or subtractive, as was subjected to the 90° phase shift in the detection dimension. The doubly phase-shifted time domain data set is then combined with the second, unshifted data set (whether added to or subtracted from is best determined by trial and error) to produce a single, signal enhanced data set which is then processed to a 2D spectrum as desired. As implied in the above discussion, performing the phase shifts in the time domain requires that the x and y components of the free induction decays be digitized at simultaneous time points and that the hypercomplex method, not TPPI, be used for sign discrimination in the relevant, indirect dimension.

To summarize in brief form, the PEP data handling procedure is as follows, assuming hypercomplex data collection:

(1a) Collect two separate data sets $u_x(t_1, t_2)$ and $v_x(t_1, t_2)$ which are identically recorded except for an inversion of the relevant phase selection pulse for the PEP scheme.

(1b) Collect a second pair of data sets $u_y(t_1, t_2)$ and $v_y(t_1, t_2)$ similarly to the first, as part of the hypercomplex procedure (12-15). (The acquisition of the four data sets u_x, v_x, u_y and v_y is normally interleaved so that four FIDs are collected before the parameter t_1 is incremented).

(2) Make the combinations $a_x = u_x + v_x$, $s_x = u_x - v_x$, $a_y = u_y + v_y$ and $s_y = u_y - v_y$.

(3) Effect a 90° phase shift in the detection dimension to create a new data set $\bar{s}_x$, $\bar{s}_y$: real($\bar{s}_x$)=imag(s_x), imag($\bar{s}_x$)=real(s_x), and the same for $\bar{s}_y$ (s_x and s_y were arbitrarily chosen over a_x and a_y).

(4) Effect a 90° phase shift in the indirect dimension to create a new data set $\tilde{s}_x$, $\tilde{s}_y$: $\tilde{s}_x$=$\bar{s}_y$ and $\tilde{s}_y$=$\bar{s}_x$.

(5) Make the combinations $c_x = a_x + \tilde{s}_x$ and $c_y = a_y + \tilde{s}_y$ (subtractive combination may be necessary instead, the uncertainty is due to hardware and pulse sequence details).

(6) Process the data $c_x(t_1, t_2)$, $c_y(t_1, t_2)$ as appropriate for a hypercomplex data set. If the TPPI procedure is used for ω_1 sign discrimination or if certain spectral editing capabilities need to be retained, then it is necessary to process the two data sets $a(t_1, t_2)$ and $s(t_1, t_2)$ separately and combine them afterward if desired.

In order to determine the sensitivity enhancement achievable using PEP methodology, it is necessary to analyze the behaviour of the signal noise (24) in these experiments. A general analysis of the noise behaviour can be performed by considering the consequences of the PEP procedure in the frequency domain. The additive and subtractive combinations of the raw, time domain data sets are made as indicated in step (2) above; no assumption is necessary regarding how the data is digitized or ω_1 frequency discrimination is achieved. The resulting two data sets are then processed separately but identically to produce two, 2D spectra, $A(\omega_1, \omega_2)$ and $S(\omega_1, \omega_2)$ (assume that only the real data has been retained and that $A(\omega_1, \omega_2)$ is phased as desired). According to the PEP protocol it is necessary to perform a 90° phase shift in each of the two frequency dimensions of one of the spectra before combining the spectra. As Ernst has pointed out (25,26), a 90° phase shift is equivalent to performing a Hilbert transformation of the data, due to the causality principle. Thus, the combined spectrum $C(\omega_1, \omega_2)$ can be written as:

$$C(\omega_1, \omega_2) = A(\omega_1, \omega_2) + \hat{S}(\omega_1, \omega_2) \qquad (12)$$

Eqn. 12 can be rewritten in expanded terms as:

$$\begin{aligned} C(\omega_1, \omega_2) &= [U(\omega_1, \omega_2) + V(\omega_1, \omega_2)] \\ &\quad + [\hat{U}(\omega_1, \omega_2) - \hat{V}(\omega_1, \omega_2)] \end{aligned} \qquad (13)$$

where $U(\omega_1, \omega_2)$ and $V(\omega_1, \omega_2)$ are the 2D spectra produced by identical processing of the original, raw data sets $u(t_1, t_2)$ and $v(t_1, t_2)$. Rearranging eqn. 13 gives

$$\begin{aligned} C(\omega_1, \omega_2) &= [U(\omega_1, \omega_2) + \hat{U}(\omega_1, \omega_2)] \\ &\quad + [V(\omega_1, \omega_2) - \hat{V}(\omega_1, \omega_2)] \end{aligned} \qquad (14)$$

Assume that the raw data consists only of random noise. In order to determine the behaviour of the spectral noise when combined according to eqn. 14, it is sufficient to calculate the cross-correlation function $R_{U\hat{U}}(\sigma_1, \sigma_2)$, where

$$R_{U\hat{U}}(\sigma_1, \sigma_2) = \mathcal{E}\{U(\omega_1, \omega_2)\hat{U}(\omega_1 + \sigma_1, \omega_2 + \sigma_2)\} \quad (15)$$

and $\mathcal{E}$ represents the mean value of the function in brackets, averaged over ω_1 and ω_2, and it is assumed that the spectral noise is stationary. The 2D Hilbert transform of $U(\omega_1, \omega_2)$ is given by (19):

$$\hat{U}(\omega_1, \omega_2) = \frac{1}{\pi^2} \int_{-\infty}^{\infty} \frac{d\alpha}{(\omega_2 - \alpha)} \int_{-\infty}^{\infty} \frac{U(\beta, \alpha)}{(\omega_1 - \beta)} d\beta \quad (16)$$

where for simplicity it is assumed that $U(\omega_1, \omega_2)$ is a continuous function and that the integration limits can be extended to infinity. Inserting eqn. 16 into eqn. 15 gives:

$$R_{U\hat{U}}(\sigma_1, \sigma_2) = \mathcal{E}\left\{\frac{1}{\pi^2} \int_{-\infty}^{\infty} \frac{d\alpha}{(\omega_2 + \sigma_2 - \alpha)} \int_{-\infty}^{\infty} \frac{U(\omega_1, \omega_2)U(\beta, \alpha)}{(\omega_1 + \sigma_1 - \beta)} d\beta\right\} \quad (17)$$

Making the substitutions $\eta = \beta - \omega_1$ and $\gamma = \alpha - \omega_2$ leads to

$$R_{U\hat{U}}(\sigma_1, \sigma_2) = \mathcal{E}\left\{\frac{1}{\pi^2} \int_{-\infty}^{\infty} \frac{d\gamma}{(\sigma_2 - \gamma)} \int_{-\infty}^{\infty} \frac{U(\omega_1, \omega_2)U(\omega_1 + \eta, \omega_2 + \gamma)}{(\sigma_1 - \eta)} d\eta\right\} \quad (18)$$

Assuming that the order of integrations can be interchanged, eqn. 18 can be expressed as:

$$\begin{aligned} R_{U\hat{U}}(\sigma_1, \sigma_2) &= \frac{1}{\pi^2} \int_{-\infty}^{\infty} \frac{d\gamma}{(\sigma_2 - \gamma)} \int_{-\infty}^{\infty} \frac{\mathcal{E}\{U(\omega_1, \omega_2)U(\omega_1 + \eta, \omega_2 + \gamma)\}}{(\sigma_1 - \eta)} d\eta \\ &= \frac{1}{\pi^2} \int_{-\infty}^{\infty} \frac{d\gamma}{(\sigma_2 - \gamma)} \int_{-\infty}^{\infty} \frac{R_{UU}(\eta, \gamma)}{(\sigma_1 - \eta)} d\eta \\ &= \hat{R}_{UU}(\sigma_1, \sigma_2) \end{aligned} \quad (19)$$

Eqn. 19 indicates that the cross-correlation function of $U(\omega_1, \omega_2)$ and its 2D Hilbert transform $\hat{U}(\omega_1, \omega_2)$ is equal to the Hilbert transform of the autocorrelation function of $U(\omega_1, \omega_2)$; this relationship is well known for functions of one variable (27,28). It is trivial to prove that $\hat{R}_{UU}(\sigma_1, \sigma_2)$ is an odd function in both σ_1 and σ_2, using the fact that $R_{UU}(\sigma_1, \sigma_2)$ is an even function by definition. Thus, since

$$\hat{R}_{UU}(-\sigma_1, \sigma_2) = -\hat{R}_{UU}(\sigma_1, \sigma_2)$$

and

$$\hat{R}_{UU}(\sigma_1, -\sigma_2) = -\hat{R}_{UU}(\sigma_1, \sigma_2)$$

it must be true that

$$\hat{R}_{UU}(0, 0) = R_{U\hat{U}}(0, 0) = 0 \quad (20)$$

Eqn. 20 indicates that a function $U(\omega_1, \omega_2)$ and its 2D Hilbert transform are uncorrelated, as is well known for 1D Hilbert transform pairs (27,29). Thus, in making the combination $U + \hat{U}$ in eqn. 17 the rms noise level increases only by a factor of $\sqrt{2}$, and the same of course is true for $V - \hat{V}$. The net result therefore is that the PEP procedure increases the spectral rms noise level by a factor of $\sqrt{2}$ over that for a conventional spectrum (corresponding to either the $U + V$ or $U - V$ combinations in eqn. 13); if the NMR signal is doubled in a PEP-modified experiment, then an improvement in sensitivity by a factor of $\sqrt{2}$ will be realized.

Perhaps the earliest example of PEP methodology was in the work of Bachmann et al. (12) on phase separation in two-dimensional spectroscopy. Two techniques were described for obtaining pure phase, 2D resolved spectra; the first technique achieved phase separation by reversed precession, while the second relied on the use of phase selection pulses between the evolution and detection periods. The reversed precession technique is really a PEP scheme, and as mentioned by Bachmann et al., provides a factor of $\sqrt{2}$ sensitivity enhancement over the phase selection method.

Before proceeding on to describe some recent applications of PEP methodology, it would perhaps be useful to point out the existence of somewhat related experiments. The PEP scheme is based on designing a pulse sequence so that the two orthogonal magnetization components present during the evolution period follow more or less equivalent coherence transfer pathways to the detection period and therefore provide essentially identical information. Other schemes have been proposed in the past which also

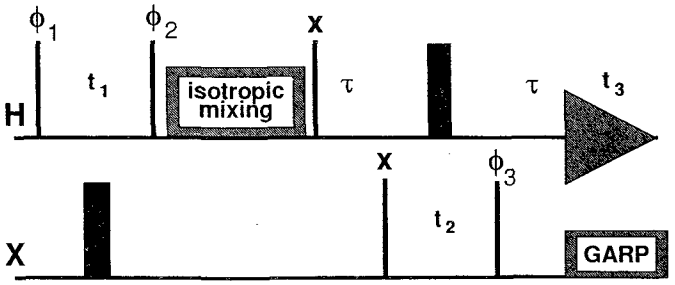

ϕ_1 = x, -x
ϕ_2 = x, x, x, x / -x, -x, -x, -x (collect data separately)
ϕ_3 = x, x, -x, -x
rec = x, -x, -x, x

Figure 2: Pulse sequence for recording 3D sensitivity-enhanced TOCSY-HMQC spectra (38). The isotropic mixing is performed using the DIPSI-2 pulse sequence (35) or other, suitable sequences. The thin and thick vertical lines represent 90° and 180° pulses, respectively, applied to the H (proton) or X (heteronucleus) spins. The delay τ is set to $1/(2J_{HX})$. Decoupling of the X spins during acquisition is accomplished using GARP-1 (54) or other appropriate composite pulse sequences. Quadrature detection in the ω_1 and ω_2 dimensions can be achieved via either the TPPI (13,16-18) or hypercomplex (12-15) methods. After the data is collected with the basic four step phase cycle (plus any additional cycling desired), the phase ϕ_2 is inverted and the resulting data set is stored separately from the first.

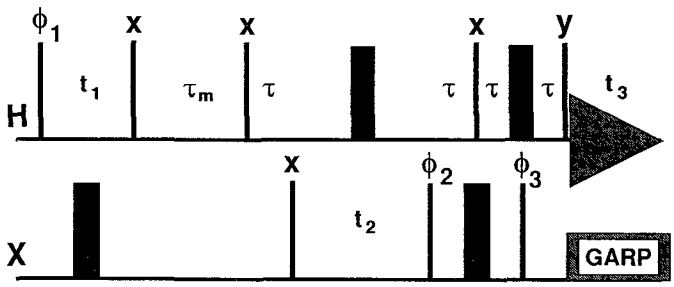

ϕ_1 = x, -x
ϕ_2 = x, x, -x, -x / -x, -x, x, x (collect data separately)
ϕ_3 = y, y, -y, -y
rec = x, -x, -x, x

Figure 3: Pulse sequence for recording 3D sensitivity-enhanced NOESY-HMQC spectra (38). The thin and thick vertical lines represent 90° and 180° pulses, respectively, applied to the H (proton) or X (heteronucleus) spins. The delay τ is set to $1/(2J_{HX})$, while τ_m is the NOE mixing period. Decoupling of the X spins during acquisition is accomplished using GARP-1 (54) or other appropriate composite pulse sequences. Quadrature detection in the ω_1 and ω_2 dimensions can be achieved via either the TPPI (13,16-18) or hypercomplex (12-15) methods. After the data is collected with the basic four step phase cycle (plus any additional cycling desired), the phase ϕ_2 is inverted and the resulting data set is stored separately from the first.

retain signals originating from the two orthogonal components in the evolution period; the difference in these schemes is that the information provided by the two signals is not the same, and thus cannot be combined to achieve a sensitivity enhancement as it is normally defined. However, when the techniques are applicable they can provide a substantial increase in the information recorded per unit measuring time. One example of such techniques is the COSY-NOESY (30) or COCONOSY (31) experiment, in which a COSY data set is recorded during the mixing time of a NOESY experiment.

Another, closely related example is the combined relayed NOESY-TOCSY experiment (32).

III. Applications

PEP technology can be applied to a wide variety of experiments (33). Brief descriptions will be given in the following sections for some representative examples of sensitivity-enhanced, solution-state NMR experiments.

1. TOCSY Experiments

Aside from the trivial case of a 2D chemical shift-resolved experiment, perhaps the simplest example of the application of PEP technology is a sensitivity-enhanced, 2D homonuclear TOCSY experiment (34). The pulse sequence for the sensitivity-enhanced TOCSY experiment is shown in Fig. 1; this sequence is just the z-filtered TOCSY experiment proposed some time ago (8,9), but with modified phase-cycling and data acquisition. Instead of phase-cycling the second 90° pulse to select for the z magnetization during the isotropic mixing period, both the z and x magnetization components are retained by performing two experiments with the phase-cycle of ϕ_2 inverted between them and the data collected separately. The two data sets are then processed according to the PEP procedure, as described above. The key to achieving sensitivity enhancement in the TOCSY experiment is to employ a mixing sequence which promotes coherence transfer with equal efficiency for the z and x magnetization components present at the beginning of the mixing period. A so-called 'isotropic' mixing sequence, such as the DIPSI-2 sequence described by Shaka et al. (35), is ideal for use in the sensitivity-enhanced TOCSY experiment; the defining characteristic of an isotropic mixing sequence is that it creates an effective Hamiltonian consisting only of the isotropic scalar coupling terms. Under such a Hamiltonian each of the orthogonal magnetization components is conserved (neglecting relaxation), since they commute with the effective Hamiltonian; thus, there is no mixing of the terms arising from the z and x magnetization present at the beginning of the mixing period. As indicated schematically in Fig. 1, z magnetization starting on one spin can be transferred to z magnetization of another spin belonging to the same coupling network, and likewise for x magnetization. In a conventional TOCSY experiment (6-9), one of these two components is intentionally destroyed in order to purge the 2D spectra of undesirable phase characteristics. With the PEP procedure, however, it has been demonstrated (34) that pure phase TOCSY spectra can be recorded with an improvement in sensitivity by a factor of $\sqrt{2}$.

2. 3D TOCSY-HMQC Experiment

The PEP sensitivity enhancement scheme can be applied in principle to a NMR experiment of any dimensionality. For example, by concatenating the 2D sensitivity-enhanced TOCSY pulse sequence with a conventional heteronuclear HMQC sequence (36,37) it is possible to create a 3D, sensitivity-enhanced TOCSY-HMQC experiment (38); this pulse sequence is shown in Fig. 2. An analysis of this relatively simple experiment shows that the two, orthogonal magnetization components created by evolution under the chemical shift interaction during the t_1 period undergo essentially identical transformations during the rest of the pulse sequence, and lead to observable signals containing equivalent information. According to the PEP prescription, two data sets are collected for each increment of t_1, with ϕ_2 being inverted between the two experiments. Data reduction is most conveniently accomplished in the time domain as the data is being accumulated.

3. 3D NOESY-HMQC Experiment

The 2D TOCSY experiment shown in Fig. 1 and the 3D TOCSY-HMQC experiment presented in Fig. 2 are examples of PEP applications in which no change in the actual pulse sequences of the corresponding, conventional experiments are required; in these cases the only changes necessary in the experimental protocol are to the phase-cycling and to the data collection procedure. This simplicity is largely due to the inherent characteristic of an isotropic mixing sequence to act on orthogonal magnetization components with equal efficiency and identical effect; in the TOCSY experiments the two equivalent coherence transfer pathways required for the PEP scheme come as a natural part of the conventional pulse sequence. However, most other multidimensional NMR experiments have one or more segments which normally treat differently the orthogonal components present at the end of a given evolution period. For example, in a 2D NOESY experiment only one of the orthogonal magnetization components present at the end of the evolution period can be converted to the longitudinal magnetization required during the NOE mixing period; the second, transverse component must be eliminated to remove coherence transfer artifacts. Thus, it is not possible to apply the PEP scheme for any evolu-

tion period which precedes a NOESY mixing period or, by analogy, a ROESY spin-lock period; however, it may be possible to apply the PEP technique to subsequent evolution periods.

Fig. 3 shows a pulse sequence for a sensitivity-enhanced, 3D NOESY-HMQC experiment (38). Unlike the TOCSY experiments, it is necessary in this case to modify the conventional sequence for this popular experiment. A detailed analysis (39,40) of the conventional HMQC experiment indicates that the two relevant, orthogonal spin operator terms present at the end of the evolution period (t_2 period in Fig. 3) are not transformed equivalently following the evolution period; one term is converted to anti-phase proton coherence which evolves into in-phase magnetization observable during the detection period, while the second term is left as unobservable multi-spin coherence and is therefore lost. However, by modifying the pulse sequence (39,40) (adding the pulses after the $90^\circ_{\phi_2}$ pulse in Fig. 3), it is possible to have both of the relevant spin operator terms from the evolution period transformed to observable magnetization for IS spin systems. While the resulting propagator does not cause the orthogonal terms to follow exactly equivalent pathways, under suitable conditions a substantial sensitivity enhancement can be achieved (39); the degree of non-equivalence is dependent on various relaxation rates. A modification analogous to that shown in Fig. 3 has also been described (39,40) for the HSQC experiment (41).

The modifications to the HMQC and HSQC experiments only allow sensitivity enhancement for IS spin systems, i.e. heteronuclear spin systems in which only one proton is directly coupled to the heteronucleus. In applications where both IS and I_nS (n>1) spin systems are present, it is sometimes useful to process separately the two data sets recorded as part of the PEP procedure; by doing so one of the two spectra will only contain resonances from the IS spin systems, while the other will contain all the resonances, thus allowing easy distinction of IS from I_nS spin systems.

4. Heteronuclear Relaxation Experiments

Over the past several years there has been a resurgence of interest in measuring heteronuclear relaxation rate constants and heteronuclear NOEs for use in studying the internal dynamics of biomolecules (42). This renaissance is due partly to the availability of methods for biosynthetically enriching biomolecules with ^{13}C and/or ^{15}N nuclei and partly due to the development of methods for indirectly measuring the heteronuclear relaxation rate constants and $\{^1H\}$-X NOEs with proton signal detection. The general scheme of the proton detection methods is to concatenate a conventional heteronuclear relaxation experiment with a HSQC experiment. For example, an experiment for measuring heteronuclear spin-spin relaxation rate constants (43,44) consists of a refocussed-INEPT (45,46) segment to enhance the sensitivity by transferring the larger proton equilibrium magnetization to the heteronuclei, a CPMG sequence (47,48) with a parametrically varied length T, and a HSQC type 2D sequence (omitting the initial INEPT segment since the desired heteronuclear coherence has already been created) to record the data. A series of 2D experiments are collected as T is varied, and a plot of the cross-peak intensities in the 2D spectra as a function of T can be analyzed as usual for CPMG experiments. If the improved resolution of a 2D correlation spectrum is unnecessary, then a simple reverse, refocussed-INEPT sequence can be used in place of the HSQC segment.

Multi-dimensional, heteronuclear NMR experiments which contain a reverse polarization transfer step lend themselves well for application of the PEP scheme (39,40). An example of a sensitivity-enhanced pulse sequence for measuring heteronuclear spin-spin relaxation rate constants is shown in Fig. 4. The section leading up to and including the t_1 evolution period is a conventional sequence, with the initial refocussed-INEPT segment, the CPMG sequence modified so that dipolar-CSA cross-correlation effects are eliminated (43,44), and the t_1 evolution period for frequency labelling the X nucleus coherences. In a conventional experiment the evolution period would be followed by a reverse polarization transfer sequence such as refocussed-INEPT or DEPT (49); these sequences transfer only one of the two, orthogonal magnetization components present at the end of the evolution period to observable proton signals. However, with relatively simple modifications (39,50), these sequences can be made to transfer both components with approximately equal efficiency to observable proton magne-

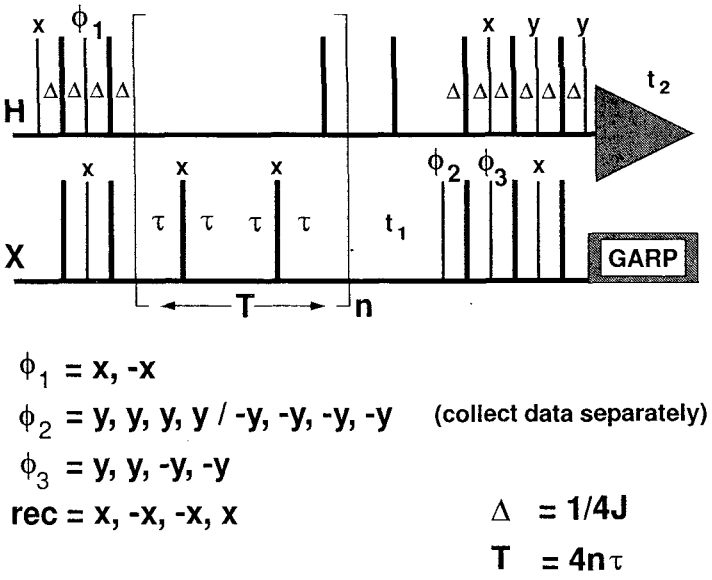

Figure 4: Sensitivity-enhanced pulse sequence for measuring heteronuclear spin-spin relaxation time constants with proton detection (50). The thin and thick bars represent 90° and 180° pulses, respectively. After the data is recorded using the basic four step phase cycle (plus any additional cycling desired), the phase ϕ_2 is inverted and a second data set is recorded separately from the first. The 180° pulses without phase designation are applied along the y axis. The value of Δ is set to $1/(4J_{HX})$. A CPMG sequence is applied to the X nucleus spins during the parametrically varied period T; the periodic proton 180° pulses applied during the CPMG sequence eliminate effects from cross-correlation between CSA and dipolar relaxation mechanisms (43,44). For each value of T a 2D X-H correlation experiment is recorded.

tization, thus allowing the PEP scheme to be implemented; in the sequence of Fig. 4 a modified, refocussed-INEPT sequence is employed. The details of these modifications have been described in detail elsewhere (39,50).

To demonstrate the use of the sensitivity-enhanced pulse sequence of Fig. 4, experimental data (Rance, Chazin and Palmer, unpublished) which was recorded for a sample of 15% uniformly, fractionally ^{13}C-enriched calbindin D_{9k} dissolved in D_2O is shown in Figs. 5 and 6. Calbindin D_{9k} is a small (76 amino acids) calcium-binding protein. Presented in Fig. 5 are contour plots of the C_α-H_α region of heteronuclear correlation spectra recorded using the pulse sequence of Fig. 4; the length of the CPMG cycle, T, was 4 ms. The data in Fig. 5a is the result of making the additive combination of the raw data recorded according to the PEP scheme, while the data in Fig. 5b results from the subtractive combination; except for a relative, 90° phase shift in both frequency dimensions, the processing and plotting parameters are identical for the two spectra. Inspection of the two contour plots shows that they are essentially identical, and thus when they are combined the sensitivity will be enhanced, since the spectral noise is uncorrelated (*vide supra*). In conventional experiments only one of these two spectra is obtained, whereas in the sensitivity-enhanced experiment both spectra are produced from the same raw data set.

Presented in Fig. 6 are 1D slices, along the proton chemical shift axis, taken from the 2D heteronuclear correlation spectra recorded with the sensitivity-enhanced pulse sequence of Fig. 4 and using a CPMG length of 108 ms. The top slice is taken from the data set representing the additive combination of the raw data, the middle slice is from the subtractive data set, and the bottom slice is the result of co-adding the two slices above. The spectra are plotted such that the rms noise level is the same

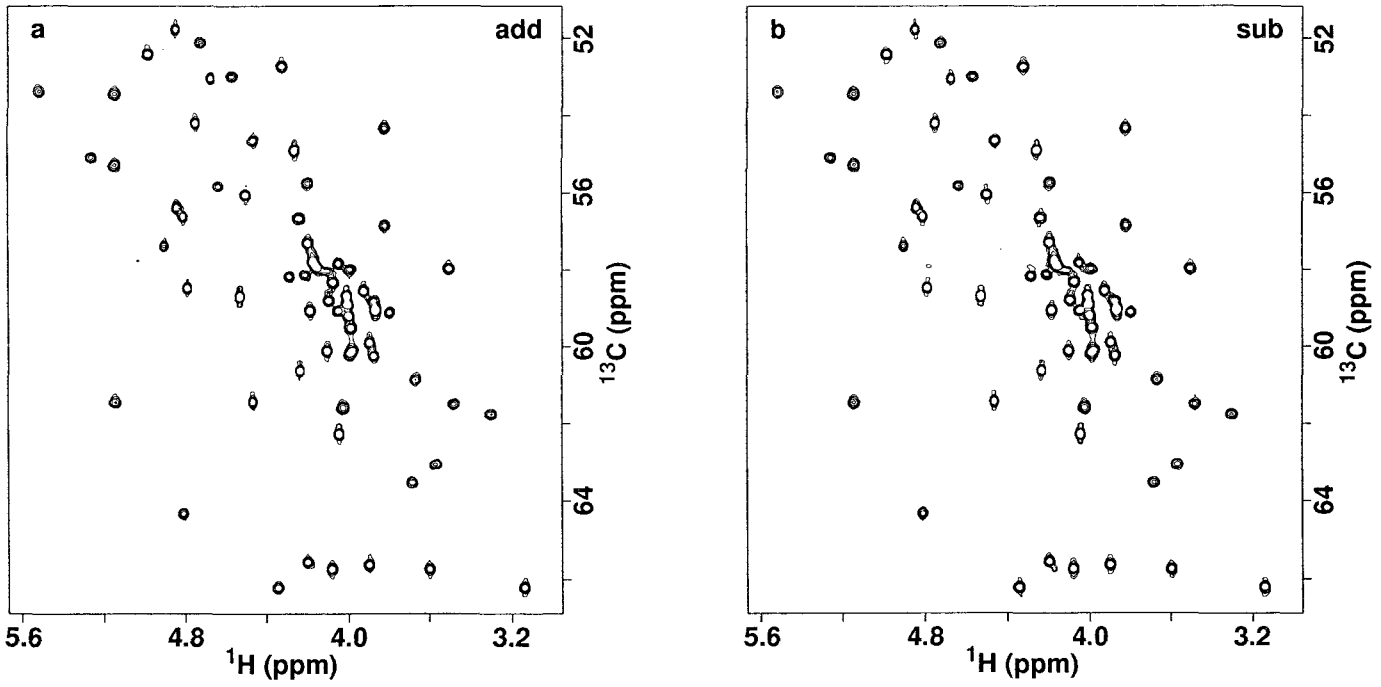

Figure 5: Contour plots of the C_α-H_α region of ^{13}C-^{1}H 2D correlation spectra for a sample of 15% fractionally ^{13}C-enriched calbindin D_{9k}, recorded using the sensitivity-enhanced pulse sequence of Figure 4 for measuring ^{13}C spin-spin relaxation time constants. The two sets of data recorded during the experiment were added together to produce plot (a) and subtracted to produce plot (b); all processing and plotting parameters were identical for the two plots except for a 90° relative phase shift in both frequency dimensions (i.e. the zeroth order phase corrections necessary for spectrum (b) were shifted by 90° from the parameters used for spectrum (a)). The length of the CPMG cycle employed in this experiment was 4 ms. All data processing was done using the FTNMR software from Hare Research.

for all slices, which required that the combined data be reduced in size by a factor of $\sqrt{2}$ before plotting with the same scaling factors as the additive and subtractive data. The sensitivity enhancement expected for the PEP scheme is clearly demonstrated by the data in Fig. 6.

5. Additional Applications

The PEP scheme is a general concept, not a specific design. In addition to the examples described above and presented in detail elsewhere (33,34,38-40), many other applications are possible. Kay and coworkers (51) have recently reported the use of PEP technology in pulsed field gradient versions of the HSQC experiment. Their new method allows pure absorption heteronuclear correlation spectra to be recorded with the use of pulsed field gradients for eliminating undesired coherence transfer pathways. PEP technology is employed in the gradient-enhanced experiment to extract separate signals which are cosine- and sine-modulated as a function of the evolution time t_1; this data can then be processed with a hypercomplex Fourier transformation to yield a pure absorption spectrum with ω_1 frequency discrimination. Madsen and Sørensen (52) have recently described very useful modifications to a variety of constant-time experiments for achieving optimal spectral resolution; PEP technology was incorporated into these experiments to enhance the sensitivity. Similarly, Madsen et al. (53) have employed the PEP scheme in designing new pulse sequences for measuring coupling constants in ^{13}C,^{15}N-labelled proteins.

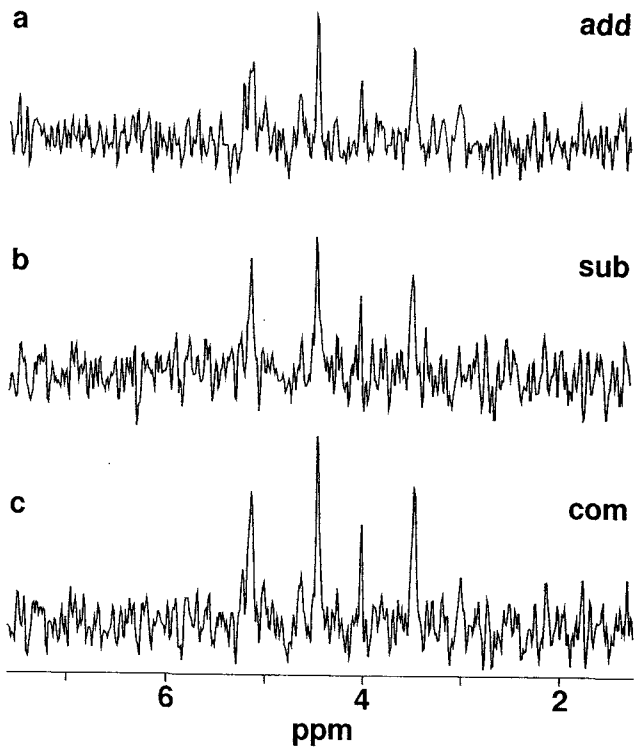

Figure 6: One-dimensional slices taken parallel to the ω_2 frequency axis (proton chemical shift) from ^{13}C-^{1}H 2D correlation spectra for the 15% fractionally ^{13}C-enriched calbindin D_{9k}; the 2D spectra were recorded using the sensitivity-enhanced pulse sequence of Figure 4 for measuring heteronuclear spin-spin relaxation time constants. The length of the CPMG cycle employed in this experiment was 108 ms. The two data sets recorded during the experiment were added together to produce the 2D spectrum from which slice (a) was taken; slice (b) is from the 2D spectrum resulting from the subtractive combination; and slice (c) is the result of co-adding slices (a) and (b). The data are plotted such that the rms noise level appears the same for all slices; this required slice (c) to be reduced in absolute terms by a factor of $\sqrt{2}$. The slices intersect peaks for the C_α-H_α correlations of Val 61 (5.10 ppm), Thr 45 (4.43 ppm), Tyr 13 (4.00 ppm), and Lys 25 (3.46 ppm).

IV. Conclusion

The general scheme of the PEP methodology for obtaining sensitivity improvements in multi-dimensional NMR experiments is simple. However, its implementation in practice may or may not be straightforward. The basic requirement which must be satisfied in order to exploit PEP technology is that the relevant, orthogonal spin operator components generated by the chemical shift/resonance offset precession during an evolution period be transformed to observable NMR signals along suitably equivalent coherence transfer pathways with approximately equal efficiency. In some applications no change in the actual pulse sequence is necessary in order to implement the PEP scheme, while other applications require some segments of the conventional pulse sequence to be re-engineered to meet the requisite conditions. It should be anticipated that PEP technology will be applicable in additional classes of experiments not specifically addressed in this paper. The maximum achievable sensitivity enhancement factor for PEP technology applied to one evolution period of a multi-dimensional NMR experiment is $\sqrt{2}$, which of course translates to a reduction by a factor of two in the measuring time required to record a data set with a given S/N ratio. Such improvement is extremely important in applications where the sensitivity is limited by practical factors such as low sample concentrations or inherent features such as the requirement for large numbers of individual free induction decays in 3D or 4D experiments or in relaxation rate measurements. Sensitivity improvements are also extremely

useful in experiments which require the data to be collected in a limited period of time.

V. Acknowledgments

I would like to acknowledge the fundamental contributions of Dr. John Cavanagh and Prof. Arthur Palmer to the development of the sensitivity-enhanced NMR experiments and the collaboration with Dr. R. Andrew Byrd on extending the original techniques to 3D applications. Helpful discussions during the course of the research with Dr. Malcolm Levitt, Prof. Geoffrey Bodenhausen and Dr. Ole Sørensen are also gratefully acknowledged. This work was supported by the National Institutes of Health (RO1-GM40089).

VI. References

[1]R.R. Ernst, *Adv. Magn. Reson.*, vol. 2, Academic Press, New York, 1966, pp. 1-135.

[2]W.P. Aue, P. Bachmann, A. Wokaun and R.R. Ernst, *J. Magn. Reson.* **29**, 523 (1978).

[3]M.H. Levitt, G. Bodenhausen and R.R. Ernst, *J. Magn. Reson.* **58**, 462 (1984).

[4]C.-N. Chen, D.I. Hoult and V.J. Sank, *J. Magn. Reson.* **54**, 324 (1983).

[5]W.P. Aue, E. Bartholdi and R.R. Ernst, *J. Chem. Phys.* **64**, 2229 (1976).

[6]L. Braunschweiler and R.R. Ernst, *J. Magn. Reson.* **53**, 521 (1983).

[7]A. Bax and D.G. Davis, *J. Magn. Reson.* **65**, 355 (1985).

[8]M. Rance, *J. Magn. Reson.* **74**, 557 (1987).

[9]R. Bazzo and I.D. Campbell, *J. Magn. Reson.* **76**, 358 (1988).

[10]M. Rance, *Chem. Phys. Lett.* **154**, 242 (1989).

[11]G. Bodenhausen, R. Freeman, R. Niedermeyer and D.L. Turner, *J. Magn. Reson.* **26**, 133 (1977).

[12]P. Bachmann, W.P. Aue, L. Müller and R.R. Ernst, *J. Magn. Reson.* **28**, 29 (1977).

[13]J. Keeler and D. Neuhaus, *J. Magn. Reson.* **63**, 454 (1985).

[14]L. Müller and R.R. Ernst, *Mol. Phys.* **38**, 963 (1979).

[15]D.J. States, R.A. Haberkorn and D.J. Ruben, *J. Magn. Reson.* **48**, 286 (1982).

[16]G. Drobny, A. Pines, S. Sinton, D. Weitekamp and D. Wemmer, *Symp. Faraday Soc.* **13**, 49 (1979).

[17]G. Bodenhausen, R.L. Vold and R.R. Vold, *J. Magn. Reson.* **37**, 93 (1980).

[18]D. Marion and K. Wüthrich, *Biochem. Biophys. Res. Commun.* **113**, 967 (1983).

[19]R.N. Bracewell, *The Fourier Transform and Its Applications*, 2nd Ed., McGraw-Hill, New York, 1986.

[20]G. Bodenhausen, H. Kogler and R.R. Ernst, *J. Magn. Reson.* **58**, 370 (1984).

[21]A.D. Bain, *J. Magn. Reson.* **56**, 418 (1984).

[22]J. Jeener, B.H. Meier, P. Bachmann and R.R. Ernst, *J. Chem. Phys.* **71**, 4546 (1979).

[23]A.A. Bothner-By, R.L. Stephens, J. Lee, C.D. Warren and R.W. Jeanloz, *J. Am. Chem. Soc.* **106**, 811 (1984).

[24]R.R. Ernst, *Rev. Sci. Instrum.* **36**, 1689 (1965).

[25]R.R. Ernst, *J. Magn. Reson.* **1**, 7 (1969).

[26]E. Bartholdi and R.R. Ernst, *J. Magn. Reson.* **11**, 9 (1973).

[27]R. Deutsch, *Nonlinear Transformations of Random Processes*, Prentice-Hall, Englewood Cliffs, New Jersey, 1962.

[28]J.S. Bendat and A.G. Piersol, *Random Data*, 2nd Ed., John Wiley and Sons, New York, 1986.

[29]R.R. Ernst and H. Primas, *Helv. Phys. Acta* **36**, 583 (1963).

[30]A.Z. Gurevich, I.L. Barsukov, A.S. Arseniev and V.F. Bystrov, *J. Magn. Reson.* **56**, 471 (1984).

[31]C.A.G. Haasnoot, F.J.M. van de Ven and C.W. Hilbers, *J. Magn. Reson.* **56**, 343 (1984).

[32]J. Cavanagh and M. Rance, *J. Magn. Reson.* **87**, 408 (1990).

[33]J. Cavanagh and M. Rance, *Ann. Reports NMR Spect.* **27**, 1 (1993).

[34]J. Cavanagh and M. Rance, *J. Magn. Reson.* **88**, 72 (1990).

[35](a) A.J. Shaka, C.J. Lee and A. Pines, *J. Magn. Reson.* **77**, 274 (1988); (b) S.P. Rucker and A.J. Shaka, *Mol. Phys.* **68**, 509 (1989).

[36]M.R. Bendall, D.T. Pegg and D.M. Doddrell, *J. Magn. Reson.* **52**, 81 (1983).

[37]A. Bax, R.H. Griffey and B.L. Hawkins, *J. Magn. Reson.* **55**, 301 (1983).

[38]A.G. Palmer, III, J. Cavanagh, R.A. Byrd and M. Rance, *J. Magn. Reson.* **96**, 416 (1992).

[39]A.G. Palmer, III, J. Cavanagh, P.E. Wright and M. Rance, *J. Magn. Reson.* **93**, 151 (1991).

[40]J. Cavanagh, A.G. Palmer, III, P.E. Wright and M. Rance, *J. Magn. Reson.* **91**, 429 (1991).

[41]G. Bodenhausen and D.J. Ruben, *Chem. Phys. Lett.* **69**, 185 (1980).

[42]A.G. Palmer, III, *Current Opinion in Biotechnology*, **4**, 385 (1993).

[43]A.G. Palmer, III, N.J. Skelton, W.J. Chazin, P.E. Wright and M. Rance, *Mol. Phys.* **75**, 699 (1992).

[44]L.E. Kay, L.K. Nicholson, F. Delagio, A. Bax and D.A. Torchia, *J. Magn. Reson.* **97**, 359 (1992).

[45]G.A. Morris and R. Freeman, *J. Am. Chem. Soc.* **101**, 760 (1979).

[46]D.P. Burum and R.R. Ernst, *J. Magn. Reson.* **39**, 163 (1980).

[47]H.Y. Carr and E.M. Purcell, *Phys. Rev.* **94**, 630 (1954).

[48]S. Meiboom and D. Gill, *Rev. Sci. Instrum.* **29**, 688 (1958).

[49]D.M. Doddrell, D.T. Pegg and M.R. Bendall, *J. Magn. Reson.* **48**, 323 (1982).

[50]N.J. Skelton, A.G. Palmer, III, M. Akke, J. Kördel, M. Rance and W.J. Chazin, *J. Magn. Reson.*, Ser. B, **102**, (in press, 1993).

[51]L.E. Kay, P. Keifer and T. Saarinen, *J. Am. Chem. Soc.* **114**, 10663 (1992).

[52]J.C. Madsen and O.W. Sørensen, *J. Magn. Reson.* **100**, 431 (1992).

[53]J.C. Madsen, O.W. Sørensen, P. Sørensen and F.M. Poulsen, *J. Biomol. NMR* **3**, 239 (1993).

[54]A.J. Shaka, P.B. Barker and R. Freeman, *J. Magn. Reson.* **64**, 547 (1985).